

Reactor Pressure Vessel Steel Embrittlement Under the Combined Action of Neutron Field and Hydrogen

Krasikov E.A.^{1,a} and Amajev A.D.^{2,b}

^{1,2}National Research Centre «Kurchatov Institute», Kurchatov sq., 1, 123182 Moscow, Russia

^aemail: ekrasikov@mail.ru, ^bemail: amajev@mail.ru

Keywords: RPV steel, embrittlement, combined action, neutron field, corrosion, hydrogen.

Abstract. As the service life of an operating nuclear power plant (NPP) increases, the potential misunderstanding of the degradation of aging components must receive more attention. Integrity assurance analysis contributes to the effective maintenance of adequate plant safety margins.

In essence, the reactor pressure vessel (RPV) is the key structural component of the NPP that determines the lifetime of nuclear power plants. Environmentally induced cracking in the stainless steel corrosion-preventing cladding of RPV's has been recognized to be one of the technical problems in the maintenance of light-water reactors. Therefore, in the case of cladding failure, the problem arises of hydrogen (as a corrosion product) embrittlement of irradiated RPV steel because of exposure to the coolant.

The effects of neutron fluence and irradiation temperature on steel/hydrogen interactions (adsorption, desorption, diffusion, mechanical properties at different loading velocities, post-irradiation annealing) were studied. Experiments clearly reveal that the higher the neutron fluence and the lower the irradiation temperature, the more hydrogen-radiation defects occur, with corresponding effects on the RPV steel mechanical properties.

Hydrogen accumulation analyses and thermal desorption investigations were performed to prove the evidence of hydrogen trapping at irradiation defects. Extremely high susceptibility to hydrogen embrittlement was observed with specimens which had been irradiated at relatively low temperature. However, the susceptibility decreases with increasing irradiation temperature. To evaluate methods for the RPV's residual lifetime evaluation and prediction, more work should be done on the irradiated metal-hydrogen interaction in order to monitor more reliably the status of RPV materials.

1. Introduction

The RPV is a large fixed structure that is subject to embrittlement and aging, the replacement of which is extremely costly. In essence, it is the condition of the RPV that determines the lifetime of nuclear power plants. Environmentally induced cracking in the stainless steel corrosion-preventing cladding of RPVs has been recognized to be one of the technical problems in the maintenance and development of light-water reactors [1]. Extensive cracking leading to failure of the cladding was found after 13 000 net hours of operation in JPDR (Japan Power Demonstration Reactor) [2]. Some of the cracks have reached the base metal and further penetrated into the RPV in the form of localized corrosion.

Failures of reactor internal components in both boiling water reactors (BWRs) and pressurized water reactors (PWRs) have increased after the accumulation of relatively high fluences ($5 \times 10^{20} \text{ cm}^{-2}$, $E \geq 0.5 \text{ MeV}$) [3]. Therefore, in the case of cladding failure, the problem arises of hydrogen embrittlement of irradiated RPV steel as a result of exposure to the coolant.

Among the principal sources of nascent hydrogen, the only significant one is the corrosion reaction at the steel/water interface [4, 5]. In this respect, in order to improve the accuracy of estimates for the remaining lifetime of an RPV, more work must be done in the irradiated metal-hydrogen interaction so that the material status of the RPV may be more reliably tracked.

2. Material and Experimental Procedures

2.1. Material and Specimens

Grade 15Cr2MoV Russian RPV steel was used in shells of VVER-440 units. The chemical composition of the material examined is given in Table 1.

Table 1. Chemical composition of 15Cr2MoVA steel [wt.%%]

C	Si	Mn	S	P	Cr	Ni	Mo	V	Cu
0.16	0.30	0.43	0.011	0.014	2.75	0.16	0.67	0.26	0.11

The heat treatment of the 15Cr2MoV samples consisted of austenization at 980–1000°C, oil quenching, tempering at 680°C, and cooling in the furnace to 350°C. After fabrication, the specimens were annealed in a vacuum furnace at 680°C.

Specimens of different types—smooth, notched, ring-shaped—(Fig.1) from the 15CrMoVA steel were placed into capsules for irradiation. Different irradiation temperatures were obtained through the inert gas gaps between the capsules and the walls of the irradiation rigs. To perform the *in-situ* corrosion-induced hydrogenation portion of the test, the specimens were irradiated in the perforated rigs.

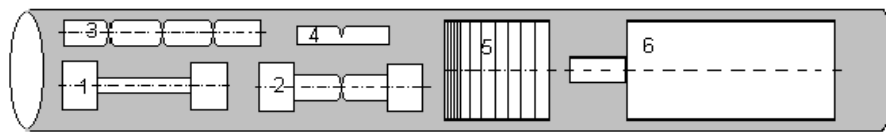


Fig.1. Diagram of the capsule arrangement, showing position of the various types of specimens: 1 - cylindrical tensile specimen; 2 - cylindrical tensile specimen with a round notch ($\rho=0,1$ mm); 3 - cylindrical specimen with three round notches ($\rho=0,25$ mm) for impact testing; 4 - three-point bend prismatic specimen with a notch ($\rho=0,1$ mm); 5 - ring-shaped specimen for tensile testing; 6 - cylindrical ring-shaped specimen for hydrogen diffusion study.

2.2. Hydrogenation

Electrolytical hydrogenation of the specimens was performed in 4% sulphuric acid. The current density was 1000A/m^{-2} , electrolyte temperature 15°C, hydrogenation times 1–140 h.

Corrosion hydrogenation during irradiation at $\approx 50^\circ\text{C}$ was accomplished by placing the specimens in contact with the water of the reactor pool.

2.3. Irradiation Conditions

Capsules were irradiated in the National Research Center “Kurchatov Institute” materials testing MR reactor at a range of temperatures from 50°C (specimens in contact with the water of the reactor pool) to 340°C (irradiation out of contact with water). The maximum fast ($E>0,5\text{MeV}$) neutron fluence of $5\times 10^{20}\text{cm}^{-2}$ was attained.

2.4. Determination of Hydrogen Content

The amounts of electrolytically introduced or corrosion-induced hydrogen were determined by vacuum thermal (up to 500°C) extraction and subsequent gas chromatography. The same apparatus was used to study the hydrogen diffusion process.

2.5. Mechanical Testing

Low-speed mechanical tests were performed on a tensile testing machine with a capacity of 10 kN at a strain rate of 10^{-3} s^{-1} .

High-speed mechanical tests were carried out on an impact testing machine with a pendulum impact velocity of $3,8 \text{ m s}^{-1}$.

To prevent hydrogen release prior to testing, hydrogenated specimens were held in liquid nitrogen.

3. Experimental Results and Discussion

3.1. Absorption, Desorption and Diffusion of Hydrogen in Irradiated Steel

Because they are responsible for hydrogen accumulation in metals under irradiation, absorption, desorption and diffusion processes have received much attention.

Figure 2 presents the plots of the dependence of electrolytic hydrogen content on neutron fluence and post-irradiation annealing. The greater the neutron fluence, the greater the hydrogen content in the metal. Generalized data on electrolytic hydrogen content vs. fast neutron fluence are presented in Fig.3. It is clearly seen that the hydrogen solubility in the irradiated specimens increases one order in comparison to unirradiated samples ($\sim 4 \text{ ppm}$).

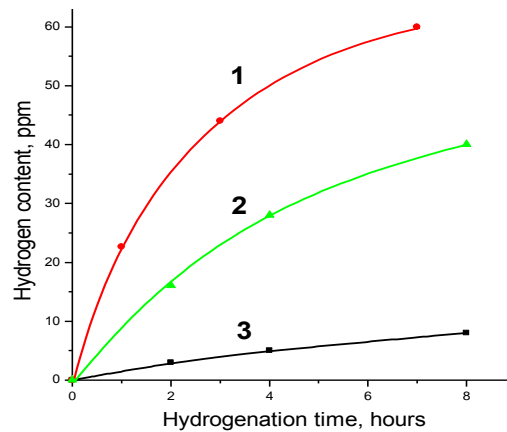


Fig.2. The kinetics of electrolytic hydrogenation of the irradiated and annealed tensile specimens: 1 - irradiated $1,7 \times 10^{20} \text{ cm}^{-2}$ at 130°C ; 2 - irradiated $4,3 \times 10^{19} \text{ cm}^{-2}$ at 180°C ; 3 - irradiated $4,3 \times 10^{19} \text{ cm}^{-2}$ at 180°C and annealed at 300°C for 1 hour. The vacuum extraction temperature was 300°C .

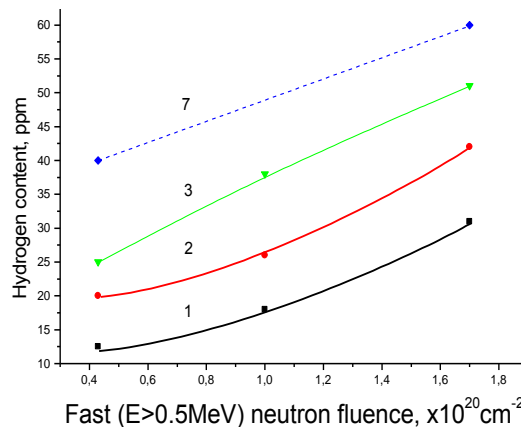


Fig. 3. Hydrogen content vs. fast neutron fluence and duration of electrolytic hydrogenation. The figures above the curves represent hydrogenation time in hours. Irradiation temperature $100\text{--}180^\circ\text{C}$.

Postirradiation annealing, on the contrary, leads to a drop in hydrogen solubility (Fig.2, curve 3). The kinetics of corrosion and electrolytic hydrogen desorption from ring-shaped samples are presented at Fig.4. One may note that low-intensity hydrogenation (i.e. corrosion) as well as electrolytically driven hydrogenation results in high hydrogen content in irradiated steel.

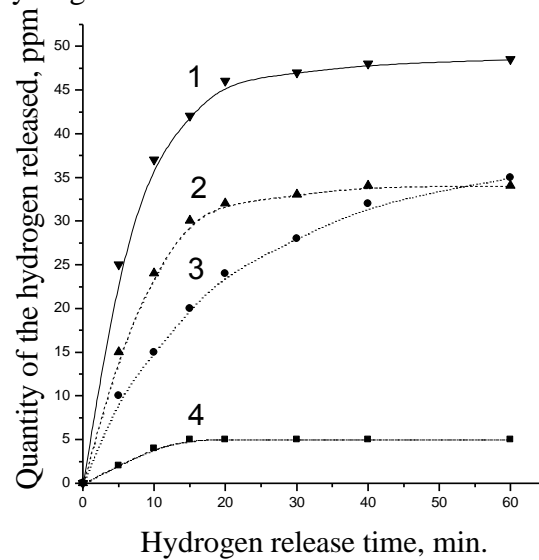


Fig. 4. The kinetics of corrosion and electrolytic hydrogen release from ring-shaped specimens. Curve 1 - represents pool water corrosion at 50°C during irradiation ($5 \times 10^{20} \text{ cm}^{-2}$), extraction at 300°C; 2 - represents irradiation up to $1 \times 10^{20} \text{ cm}^{-2}$ and electrolytic hydrogenation (3 hours), with extraction at 300°C; 3 - represents pool water corrosion at 50°C during irradiation ($5 \times 10^{20} \text{ cm}^{-2}$), extraction at 250°C; 4 - represents electrolytic hydrogenation (3 hours) of the unirradiated specimen, extraction at 300°C.

Experiments on hydrogen diffusion through the walls of the cylindrical ring-shaped specimens were carried out. Results of the influence of irradiation and post-irradiation annealing on electrolytic hydrogen diffusion and penetration through the 1 mm wall are presented in Fig.5. The values of the hydrogen diffusion coefficients obtained by the Barrar method [6] are given in Table 2.

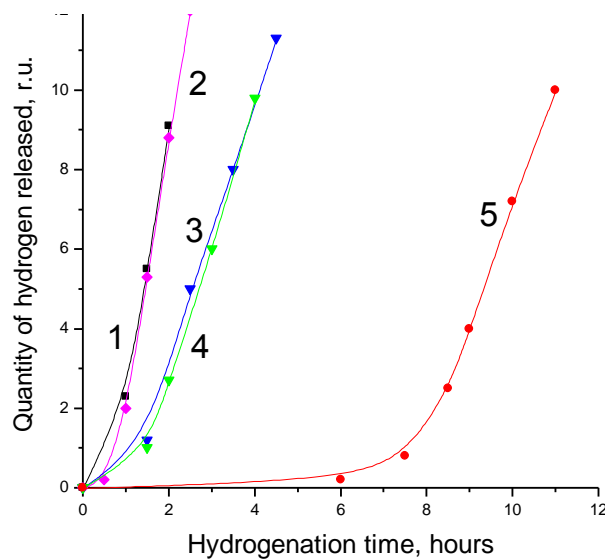


Fig.5. Quantity of hydrogen penetrated during diffusion through the 1 mm wall of the cylindrical ring-shaped specimen vs. hydrogenation time. Curves 1 and 2 represent two sets of data from the hydrogenation of the same unirradiated specimens; 3 - irradiation up to $1 \times 10^{20} \text{ cm}^{-2}$ at 100°C and annealing at 250°C; 4 - irradiation up to $1 \times 10^{20} \text{ cm}^{-2}$ at 100°C and annealing at 300°C; 5 - irradiation up to $1 \times 10^{20} \text{ cm}^{-2}$ at 100°C. The annealing time for all specimens was 1 hour.

Table 2. Influence of irradiation at 100°C and post-irradiation annealing on the hydrogen diffusion

Thickness of specimen wall, [mm]	Neutron fluence, $\times 10^{20} [\text{cm}^{-2}]$	Annealing temperature, [°C]	Diffusion coefficient, $\times 10^{-7} [\text{cm}^2 \text{s}^{-1}]$	Extraction temperature, [°C]	Hydrogen content, [ppm]
1	0	-	6,9	200	5
	1	-	0,6	200	33
		200	2,1	250	24
		250	4,2	300	12
		300	4,2	300	6
2	0	-	9,2	200	5
	1	-	1,2	200	44
		200	2,5	250	28
		250	5,6	300	15
		300	7,1	300	9
4	0	-	8,9	200	8
	1	-	1,1	200	41
	5	-	0,8	200	39

3.2. Influence of Hydrogen on Mechanical Properties of Irradiated and Annealed Steel

The approach generally adopted to characterize hydrogen embrittlement is based on extensive mechanical testing. The degree of hydrogen embrittlement depends strongly on the stress mode and/or on deformation speed. That is why different kinds of mechanical tests and specimens types are used.

3.2.1. Mechanical Properties Determined In Static Tests

3.2.1 a) Tension

Table 3 contains data on the influence of hydrogenation on tensile properties of unirradiated and irradiated smooth and notched specimens. It follows from these results that hydrogenation can slightly modify strength parameters, but it leads to a drastic decrease in plasticity. This effect is particularly pronounced for notched specimens. Thus, any imperfections of the metal structure must affect the degree of the hydrogen embrittlement. This effect is further enhanced by neutron irradiation, during which the plasticity characteristics may drop to zero. It must be emphasized that hydrogenation of the heavily irradiated notched specimens retards the strength of the material (from 1380 MPa down to 614 MPa)—a potentially dangerous tendency.

Important information can be gained from Table 4, where the influence of repeated cycles of “hydrogenation/annealing” on neutron irradiated steel is presented. It is obviously seen that cycling treatment reduces the plasticity and strength of the material. Thus in transient regimes of the nuclear power plant operation, the development of hydrogen embrittlement of the RPV steel is more probable. At the same time, it is seen from Table 4 that post-irradiation annealing practically fully eliminates the consequences of a single “irradiation+hydrogenation” episode.

3.2.1 b) Bending

Figure 6 shows load-strain diagrams for three-point bend tests of the irradiated, irradiated/annealed, and hydrogenated prismatic specimens. Again, these studies suggest the existence of residual (unrecovered by annealing) degradation effects caused by hydrogenation, as indicated earlier for the smooth and notched tensile specimens.

Table 3. Influence of neutron irradiation and hydrogenation on tensile properties

unirradiated specimens						
Hydrogenation time, [hours]	H content, [ppm]	Smooth specimens			Notched specimens	
		Ultimate tensile strength, [MPa]	Yield strength, [MPa]	Elongation, [%]	Ultimate tensile strength, [MPa]	Deformation, [%]
0	1,2	563	411	25,5	89,5	1,1
4	5,1	605	465	21,2	88,1	0,5
10	4,5	608	471	16,8	83,3	0,3
irradiated specimens						
Smooth specimens were irradiated at $4,3 \times 10^{19} [\text{cm}^{-2}]$ and $180 [^{\circ}\text{C}]$ Notched specimens were irradiated at $2,3 \times 10^{19} [\text{cm}^{-2}]$ and $170 [^{\circ}\text{C}]$						
0	0	721	711	16,2	1082	0,6
4	30	805	802	6,1	1051	0,1
14	45	772	683	2,4	1038	0
irradiated specimens						
Smooth specimens were irradiated at $1,7 \times 10^{20} [\text{cm}^{-2}]$ and $130 [^{\circ}\text{C}]$ Notched specimens were irradiated at $1,9 \times 10^{20} [\text{cm}^{-2}]$ and $125 [^{\circ}\text{C}]$						
0	0	884	858	9,1	1380	0,2
1	30	912	842	3,2	1270	0
3	51	766	766	0	890	0
7	60	840	840	0,2	614	0

Table 4. Influence of neutron irradiation ($4,3 \times 10^{19} [\text{cm}^{-2}]$ at $180 [^{\circ}\text{C}]$) and repeated cycles of hydrogenation and annealing (at $300 [^{\circ}\text{C}]$ for 1 hour) on tensile properties of smooth specimens

Hydrogenation [hours]	Annealing	Repeat hydrogenation, [hours]	Repeat annealing	Ultimate tensile strength, [MPa]	Yield strength, [MPa]	Elongation, [%]
4	+	-	-	675	576	23,3
4	+	4	+	624	482	13,6
8	+	8	+	587	477	9,8

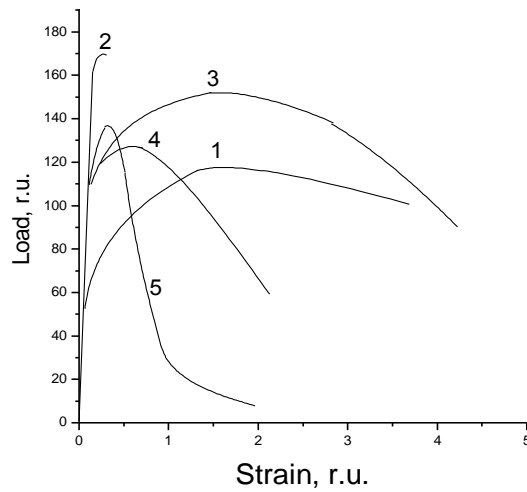


Fig.6. Load-strain diagrams (relative units) for three-point bend tests of the prismatic irradiated/annealed, hydrogenated specimens. Curve 1 represents the initial (unirradiated) condition; 2 - irradiation up to $2,7 \times 10^{20} \text{ cm}^{-2}$ at 125°C ; 3 - irradiation up to $2,7 \times 10^{20} \text{ cm}^{-2}$ at 125°C and annealing; 4 and 5 - irradiation up to $2,7 \times 10^{20} \text{ cm}^{-2}$ at 125°C , annealing, hydrogenation (20 ppm) and re-annealing. All specimens were annealed at 300°C for 1 hour.

3.2.2. Mechanical Properties Determined in Dynamic (Impact) Tests

Unirradiated metals subject to dynamic tests usually do not respond to hydrogenation, i.e. dissolved hydrogen does not keep pace with the tip of the fast moving crack. Figure 7 shows the pronounced additional embrittlement caused by the hydrogenation of steel irradiated at “low” ($140\text{-}180^\circ\text{C}$) temperatures. Alternatively, for steel irradiated at “high” (340°C) temperature, this effect does not occur, even after repeated hydrogenation/annealing cycles.

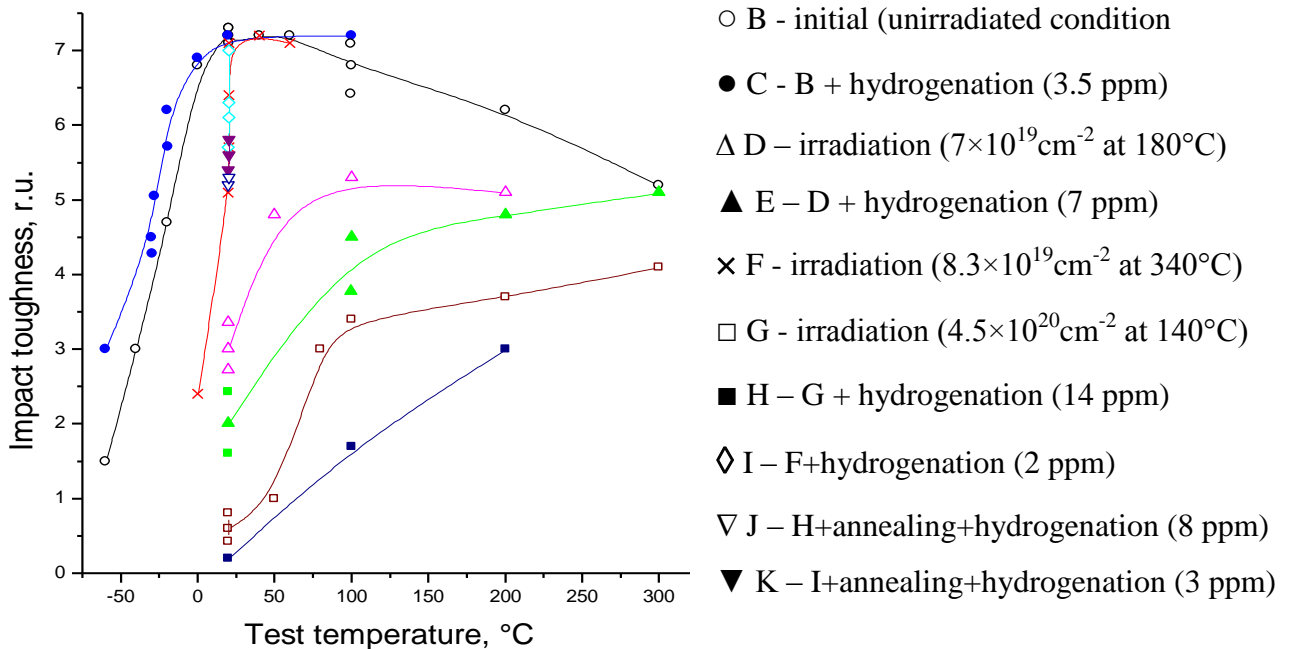


Fig.7. Impact toughness (relative units) vs. test temperature for irradiated, irradiated/annealed, and hydrogenated steel. Samples were annealed at 300°C for 1 hour.

Thus, RPV steel irradiated at relatively high ($\approx 300^\circ\text{C}$) temperature (i.e. close to the routine operating temperature of PWRs) may be immune to hydrogen embrittlement. This finding is confirmed by the data on probes (templets) taken from the functioning unclad RPVs [7] and also data received by German specialists [8].

4. Conclusions

4.1. Neutron irradiation of RPV steel at relatively low temperatures can increase by several factors the hydrogen solubility. Experiments clearly reveal that the greater the neutron fluence, the greater the hydrogen content in the metal, with a one-order increase of the hydrogen solubility in an irradiated metal, compared to an unirradiated sample.

4.2. Postirradiation annealing, on the contrary, leads to a drop in hydrogen solubility. In this respect, it is worthwhile to treat periodically structural materials subject to irradiation at temperatures up to 200°C by annealing at higher temperatures.

4.3. The low-intensity hydrogenation (i.e., corrosion) as electrolytically driven hydrogenation results in a high hydrogen content in irradiated steel.

4.4. For 15Cr2MoVA steel irradiated at 340°C, the quantity of electrolytically introduced hydrogen is lower not only than that for steel irradiated at 50-180°C, but also for the unirradiated metal as well.

4.5. Irradiation of the steel within the temperature range of 50–180°C leads to a sharp decrease of the hydrogen diffusion coefficient. Radiation-induced defects act as hydrogen traps. Postirradiation annealing causes the recovery of the hydrogen diffusion coefficient, but a residual effect persists even after heat treatment at 300°C.

4.6. From the results of experiments using smooth and notched specimens, mechanical tests show that hydrogenation slightly modifies strength parameters but can lead to a drastic decrease of plasticity. This effect is particularly pronounced for notched specimens. Thus, imperfections of the metal's structure must affect the degree of hydrogen embrittlement. This effect is further enhanced by neutron irradiation, during which the plasticity after hydrogenation may drop to zero.

4.7. Repeated treatment cycles of hydrogenation/annealing for neutron irradiated steel has a negative effect on the plasticity of the material - a potentially dangerous tendency. Therefore the development of hydrogen embrittlement of RPV steel in transient regimes of operation is probable.

4.8. Dynamic (impact) tests of steel irradiated at 140–180°C are affected by hydrogenation; i.e. hydrogen modified the parameters of radiation defects. Alternatively for metals irradiated at “high” (~340°C) temperatures, this effect does not occur, even after repeated hydrogenation/annealing cycles. So, on preliminary examination, it may be noted that RPV steel irradiated at relatively high (~300°C) temperatures (i.e. close to the routine operating temperatures of the PVRs) is immune to hydrogen embrittlement that was confirmed later.

References

- [1] E.A. Wimunc. How Serious Are Vessel Cladding Failures? Power Reactor Technology Vol.9 (1966) p.101-109.
- [2] T. Kondo, H. Nakajima and R. Nagasaki. Metallographic Investigation on the Cladding Failure in the Pressure Vessel of a BWR. Nuclear Engineering and Design Vol.16 (1971) p.205-222.
- [3] Environmentally Assisted Cracking in Light Water Reactors. NUREG/CR-4667, ANL-95/41, Vol.20, 1995.
- [4] D.R. Harries and G.H. Broomfield. Hydrogen Embrittlement of Steel Pressure Vessels in Pressurized Water Reactor Systems. Journal of Nuclear Materials Vol.9 (1963) p.327-338.
- [5] N.N. Alekseenko, A.D. Amaev, I.V. Gorynin, V.A. Nikolaev, Radiation Damage of NPP Pressure Vessel Steels, American Nuclear Society, La Grande Park, Illinois, USA, 1997.
- [6] R.M. Barrar. Philosophical Magazine Vol.28 (1939) p.139-152.
- [7] P. Platonov, Ja. Shtrombakh et.al. Results on research of templates from Kozloduy-1 RPV. Nuclear Engineering and Design Vol.191 (1999) p.313-325.
- [8] G. Müller, M. Uhlemann, A. Ulbricht and J. Böhmert. Influence of hydrogen on the toughness of irradiated RPV steels. Journal of Nuclear Materials Vol.359 (2006) p.114-121.